2005

pH-Dependent Substrate Preference of Pig Heart Lipoamide Dehydrogenase Varies with Oligomeric State: Response to Mitochondrial Matrix Acidification

Natalia L. Klyachko
M. V. Lomonosov Moscow State University, 119899 Moscow, Russia

Valentina A. Shchedrina
University of Nebraska - Lincoln, vshchedrina2@unl.edu

Alexander V. Efimov
Institute of Protein Research of Russian Academy of Sciences, Puschino-on-Oka, Moscow Region, Russia

Sergey V. Kazakov
Department of Chemistry and Physical Sciences, Pace University, Pleasantville, New York

Irina G. Gazaryan
Burke Medical Research Institute, White Plains, New York 10605

See next page for additional authors

Published in *Journal of Biological Chemistry* 280:16 (April 22, 2005), pp. 16106-16114; doi: 10.1074/jbc.M414285200

This work was supported by NATO Grant LST.CLG.978592 (to A. M. B. and N. L. K.) and National Institutes of Health NINDS Grant NS38741 (to A. M. B.). The Dyson College of Arts and Sciences, Pace University, provided start-up funding for S. V. K.

Submitted December 20, 2004; revised February 14, 2005; published online February 14, 2005.

pH-dependent Substrate Preference of Pig Heart Lipoamide Dehydrogenase Varies with Oligomeric State: Response to Mitochondrial Matrix Acidification

Natalia L. Klyachko,[1] Valentina A. Shchedrina,[1] Alexander V. Efimov,[2] Sergey V. Kazakov,[3] Irina G. Gazaryan,[4,5] Bruce S. Kristal,[4,5] and Abraham M. Brown [4,6]

[1] Department of Chemical Enzymology, M. V. Lomonosov Moscow State University, 119899 Moscow, Russia
[2] Institute of Protein Research of Russian Academy of Sciences, Puschino-on-Oka, Moscow Region, Russia
[3] Department of Chemistry and Physical Sciences, Pace University, Pleasantville, New York 10570
[4] Burke Medical Research Institute, White Plains, New York 10605
[5] Department of Neurology and Neuroscience, Weill Medical College of Cornell University, New York, New York 10021
[6] Department of Biochemistry, Weill Medical College of Cornell University, New York, New York 10021
Corresponding author – A. M. Brown, Dementia Research Service, Burke Medical Research Institute, 785 Mamaroneck Ave., White Plains, NY 10605; tel 914 597-2327, fax 914 597-2757, email ambrown@med.cornell.edu

Abstract

Cycling of intracellular pH has recently been shown to play a critical role in ischemia-reperfusion injury. Ischemia-reperfusion also leads to mitochondrial matrix acidification and dysfunction. However, the mechanism by which matrix acidification contributes to mitochondrial dysfunction, oxidative stress, and the resultant cellular injury has not been elucidated. We observe pH-dependent equilibria between monomeric, dimeric, and a previously undescribed tetrameric form of pig heart lipoamide dehydrogenase (LADH), a mitochondrial matrix enzyme. Dynamic light scattering studies of native LADH in aqueous solution indicate that lowering pH favors a shift in average molecular mass from higher oligomeric states to monomer. Sedimentation velocity of LADH entrapped in reverse micelles reveals dimer and tetramer at both pH 5.8 and 7.5, but monomer was observed only at pH 5.8. Enzyme activity measurements in reverse Aerosol OT micelles in octane indicate that LADH dimer and tetramer possess lipoamide dehydrogenase and diaphorase activities at pH 7.5. Upon acidification to pH 5.8 only the LADH monomer is active and only the diaphorase activity is observed. These results indicate a correlation between pH-dependent changes in the LADH reaction specificity and its oligomeric state. The acidification of mitochondrial matrix that occurs during ischemia-reperfusion injury is sufficient to alter the structure and enzymatic specificity of LADH, thereby reducing mitochondrial defenses, increasing oxidative stress, and slowing the recovery of energy metabolism. Matrix acidification may also disrupt the quaternary structure of other mitochondrial protein complexes critical for cellular homeostasis and survival.

Abbreviations: I/R, ischemia-reperfusion injury; AOT, Aerosol OT or sodium *bis*(2-ethylhexyl)sulfosuccinate; DCPIP, 2,6-dichlorophenolindophenol; LA, oxidized lipoamide; LADH, lipoamide (dihydrolypoil) dehydrogenase; PDHC, pyruvate dehydrogenase complex; DLS, dynamic light scattering.

Transient ischemia results in cellular necrosis and depressed cellular activity that often precedes apoptotic death, which is referred to as ischemia-reperfusion injury (I/R). Coupled mitochondria maintain a pH gradient such that its internal, or matrix, pH is more alkaline than the cytosol (1, 2). Loss of mitochondrial membrane potential, which occurs during ischemia, results in matrix acidification (3, 4). Anaerobic energy metabolism causes the accumulation of cytosolic lactic acid, which might further contribute to matrix acidification. It is well documented that substrate flux through the energy-producing mitochondrial pyruvate dehydrogenase complex (PDHC) is reduced for up to 24 h after I/R in either heart (5, 6) or brain (7–10). Cytosolic pH cycling has been linked to I/R-induced impairment of mitochondrial function (11) and, in particular, to reduced PDHC activity (8, 10, 12, 13). However, a biochemical mechanism for the persistent mitochondrial dysfunction observed in the cells that survive I/R has not been elucidated.

PDHC is composed of three enzymes catalyzing a series of sequential reactions (14). The final reaction in this sequence, reduction of NAD^+ to NADH, is catalyzed by lipoamide dehydrogenase (LADH). LADH (EC 1.8.1.4 [EC]) belongs to the family of FAD-dependent thiol-disulfide oxidoreductases, which include glutathione and thioredoxin reductases (15). LADH is a dimeric flavoprotein with subunit molecular mass of 52 kDa that contains one molecule of FAD and a catalytically active disulfide bridge per subunit (16). LADH also catalyzes a "diaphorase" reaction, *i.e.* reduction of quinones by NADH, and a mechanistically related oxidase reaction that generates superoxide and hydrogen peroxide. We have demonstrated previously that Zn^{2+} inhibits the thiol-disulfide oxidoreductase activity of LADH, whereas it enhances the oxidase activity (17). In this example, the optimal conditions for dehydrogenase and oxidase reactions catalyzed by LADH are mutually exclusive. Similarly, earlier studies reported different pH optima for dehydrogenase (18, 19) and diaphorase activities (20). Thus pH may provide another potentially physiological way to modify LADH catalytic activity.

Published results suggest that LADH exists as a stable dimer. Chemical modification allowed the preparation of monomer, which was reported to retain diaphorase activity (21). In addition, conformational instability of the fully reduced LADH from *Azotobacter vinelandii* has been reported (22). We have observed

inactivation of LADH under reducing conditions, which was favored under more dilute conditions (I. G. Gazaryan and A. M. Brown, unpublished results). This suggests that dissociation of the pig heart LADH dimer may be involved in the inactivation process.

The tendency toward higher oligomeric association of LADH is suggested by the binding of its dimer to the core structures of several enzyme complexes (23). Size exclusion chromatography of concentrated purified LADH provided evidence for tetrameric LADH, as shown below. Taken together, these observations suggested that LADH might exist as monomer, dimer, and tetramer in solution.

Precise knowledge of the catalytic properties of different oligomeric forms of LADH and conditions that promote their interconversion may be of key importance for understanding intracellular changes in PDHC activity. The goal of this work was to characterize the pH dependence of the enzymatic activities and oligomerization of pig heart LADH. Physical and enzymatic studies indicate that substantial changes in both the degree of oligomerization and the catalytic specificity of LADH occur over a narrow, physiologically important pH range. The possible role of pH changes associated with I/R in the alteration of LADH activity or other mitochondrial functions is discussed.

Materials and Methods

Reagents

NADH, Tris, 2,6-dichlorophenolindophenol (DCPIP), and citric acid were from Sigma. NaOH, HCl, and acetonitrile were purchased from Reakhim (Russia). Me_2SO was from Amerco, D,L-α-lipoamide was from Lancaster Synthesis (Great Britain). All solutions were prepared using Milli-Q water with >15 MΩ/cm resistance. All reagents were "ultra grade," if available, to reduce the possibility of divalent cation contamination.

NADH and DCPIP (ε_{600} = 20,600 M^{-1} cm^{-1}, pH 7.0 (24)) stock solutions (50 and 13–16 mM , respectively) were prepared daily in Tris-HCl, pH 7.5, or citrate, pH 5.8, buffer solutions. *n*-Octane (analytical grade, Reakhim) was treated with H_2SO_4 followed by treatment with Na_2CO_3 and a subsequent distillation. *Bis*-(2-ethylhexyl)sodium sulfosuccinate (AOT) (ultra grade) was purchased from American Cyanamid Co. LADH from porcine heart (Type III) was from Sigma.

Methods

Enzyme Preparation – LADH suspension in 3.2 M ammonium sulfate (500 μl) was centrifuged at 9,000 x *g* for 5 min on a Eppendorf MiniSpin centrifuge, the supernatant was discarded and the pellet dissolved in 500 μl of 50 mM Tris-HCl buffer, pH 7.5, or 25 mM citrate buffer, pH 5.8. The remaining ammonium sulfate was removed by gel-filtration through a Sephadex G-25 column (NAP-5; Amersham Biosciences) pre-equilibrated with 50 mM Tris-HCl buffer, pH 7.5, or 25 mM citrate buffer, pH 5.8. The concentration of the eluted protein was determined spectrophotometrically using the extinction coefficient of ε_{455} = 11,300 M^{-1} cm^{-1} (25, 26). The A_{280}/A_{455} ratio of the enzyme preparations obtained was 5.3–5.8.

Fast Protein Liquid Chromatography of Porcine Heart LADH – Chromatography was performed on a Superdex 200 column (Amersham Biosciences) equilibrated with 0.2 M Tris-HCl buffer, pH 7.5. An aliquot of LADH suspension was diluted 3-fold in water, filtered through a 0.22-μm filter, and then 1 ml (about 4 mg of protein) of the resulting solution was applied to the column. Optical density was recorded with a flow-through cell at 280 nm and eluting fractions were collected. LADH activity in collected fractions was measured with 0.2 mM lipoamide and 0.1 mM NADH in 50 mM Tris-HCl buffer, pH 7.5. NADH oxidation was monitored by absorbance at 340 nm in a 96-well plate reader (SpectraMax Plus, Molecular Devices). The reaction was initiated by the addition of LADH.

Dynamic Light Scattering (DLS) – Light scattering measurements were carried out on a "PhotoCor Complex" Photon Correlation Spectrometer (PhotoCor Instruments Inc., College Park, MD) utilizing a 20-milliwatt He-Ne laser as a light source. All measurements were performed at 25.0 ± 0.1 °C. The thermostatted bath and the cell holder were coaxial with *z* axis of a precise goniometer. The photo-detecting system comprised efficient receiving optics, a low-noise photomultiplier tube operating in a photon counting regime, and an amplifier discriminator. A single-board digital correlator analyzed the output signal of the photo-detecting system using a programmable number of channels in linear (128) and multi-tau (256) regimes. Scattering measurements were done at 30 and 90°. Particle size distribution analysis was carried out with the DynaLS version 2 program (Alango Ltd., Haifa, Israel).

Diaphorase Activity of LADH in Reverse AOT Micelles in n-Octane – The most commonly used system for preparation and study of reverse micelles is water/AOT/octane, which forms optically transparent and stable solutions of spherical reverse micelles (27). In the case of AOT reverse micelles, the particle size distribution is narrow, *i.e.* uniformed micelles of equal size are formed at each surfactant hydration degree, $w_o = [H_2O]/[AOT]$ (28, 29). The inner cavity radius of the micelle, r_m, expressed in Å, was shown to conform to the empirical equation (27),

$$r_m = 1.5\, w_0 + 4 \quad (1)$$

which holds for all enzyme-containing reverse AOT micellar systems studied thus far (29).

In a typical kinetic experiment, a solution of LADH, NADH, and DCPIP in 50 mM Tris-HCl buffer, pH 7.5, or in 25 mM citrate buffer, pH 5.8, was solubilized by intensive shaking in a solution of 0.1 M AOT in octane. The surfactant hydration degrees, w_o, were varied over the range of 12–46. The final reagent concentrations were 25–300 nM LADH, 0.01–0.75 mM NADH, and 0.003–0.15 mM DCPIP. The total volume of the reaction mixture was 2 ml. The background rate for non-enzymatic reduction of DCPIP by NADH was subtracted from the reaction rate values measured in the presence of the enzyme.

All activity measurements were performed on a Shimadzu UV-1601PC spectrophotometer (Shimadzu Corp., Kyoto, Japan) equipped with a cell holder thermostatted at 25 °C and a light path of 1 cm. The reaction was monitored by DCPIP absorbance changes. The extinction coefficient of DCPIP in reverse AOT micelles in octane differs from that in water. DCPIP spectra were scanned at hydration degrees, w_o, in the range 12–44 and in the pH range of 5.8–8.5. The extinction coefficients were determined to be 12,730 M^{-1} cm^{-1} for Tris-HCl buffer, pH 7.5 (λ_{max} = 568 nm), and 11,300 M^{-1} cm^{-1} for citrate buffer, pH 5.8 (λ_{max} = 535 nm). To determine V_m and K_m values, DCPIP concentration was varied at a saturating concentration (0.225 mM) of NADH.

The kinetic parameters V_m and K_m were calculated from kinetic curves by using the Michaelis-Menten equation, $v = V_m[S]_0/K_m + [S]_0$, where v is the rate of reaction; V_m is the observed maximal rate of the reaction; K_m is the observed Michaelis constant and $[S]_0$ is the initial concentration of substrate.

Lipoamide Dehydrogenase Activity of LADH in Reverse AOT Micelles in n-Octane – All activity measurements were performed as above, except the reaction time course was monitored by NADH absorbance decrease at 340 nm. To determine V_m and K_m values, lipoamide (LA) concentration was varied at a fixed concentration (0.1 mM) of NADH. LA was diluted from a 1 M stock in Me_2SO. As in the case with DCPIP, acetonitrile was added to the micellar system to improve solubilization at high hydration degrees of the reagent (w_o = 30–42). The final reagent concentrations were in the range of 40–300 nM LADH, 0.1 mM NADH, and 0.25–2 mM LA. The final combined concentration of Me_2SO and acetonitrile was less than 5% of the water phase volume in the micellar system.

Sedimentation Measurements – Sedimentation coefficients, *s*, of empty and LADH-containing reverse AOT micelles were determined in 12-mm bisection cells at 20 °C using a Beckman E analytical ultracentrifuge, fitted with a photoelectric scanning device, monochromator, and a multiplexor, and an An-G-Ti rotor at 20,000 rpm as previously described (30, 31). Absorbance scanning was carried out at 280 nm. Aqueous solutions of LADH in Tris-HCl buffer, pH 7.5, or in citrate buffer, pH 5.8, were solubilized in 0.1 M AOT in octane at different hydration degrees, w_o = 12–44. The protein concentrations were 5–10 μM. Prior to sedimentation experiments, the micellar solutions were incubated at room temperature for 0.5–1 h. The dependence of *s* on w_o was analyzed as previously described (31). The values of molecular masses of protein forms incorporated into reverse micelles, M_P, were calculated from the *s* values according to the empirical equation (31),

$$M_P = M_0(S_P/S_0 - 1)\cdot(1 - \rho\bar{V}_0) \quad (2)$$

where M_0 is a molecular mass of enzyme-free (empty) micelles; S_P and S_0 are sedimentation coefficients of protein-containing and empty micelles, respectively; $\bar{V}_0$ is the partial molar volume of empty micelles in the solvent with density ρ.

Computer Modeling – The three-dimensional structures of monomeric,

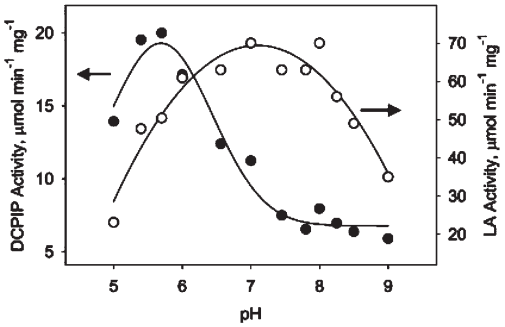

Figure 1. pH dependence of diaphorase (•) and lipoamide dehydrogenase (○) reactions catalyzed by pig heart LADH. Reaction conditions were: DCPIP, 0.1 mM ; NADH, 0.05 mM ; LADH, 50 nM; extinction coefficient for DCPIP at 510 nm, 7.5 mM^{-1} cm^{-1}; or LA, 0.2 mM , NADH, 0.1 mM , LADH, 10 nM; at 22 °C, 50 mM Tris, pH 7.4.

dimeric, and tetrameric forms of pig LADH were obtained by homology modeling. First, homologous proteins with known three-dimensional structures were identified using BLAST (32). Pairwise sequence alignment indicated that garden pea LADH (Protein Data Bank code 1DXL [PDB]) is one of the best potential templates for homology modeling of pig heart enzyme (GenBank™ 118675, SwissProt Database code P09623 [GenBank]). Pig heart LADH has 57% conserved and 74% semi-conserved amino acids compared with pea LADH sequence. This conclusion was supported by multiple sequence alignment performed with the CLUST-ALW program (33). An additional consideration in choosing pea garden LADH as the modeling template is that it occurs in tetrameric form in the asymmetric unit of LADH crystal. A structural model of pig heart LADH was built using the program on the SWISS-MODEL server (34). Visual analysis of the models obtained was performed with a DeepView/Swiss-Pdb Viewer, version 3.7 (35).

Results

pH Dependence of Lipoamide and Diaphorase Activities – The pH dependence of the activity of pig heart LADH in NADH-dependent reduction of LA (Figure 1) displays a broad activity maximum at pH 6.5–8, which is in agreement with earlier reports (18, 19). Diaphorase activity was monitored as the NADH-dependent reduction of DCPIP. The preference for the LA reaction over DCPIP varies from 3 to 9 as pH increases from 6 to 8. The optimum DCPIP activity was centered below pH 6 (Figure 1), which is in agreement with measurements done using benzoquinone (20), ferrycianide (20), and oxygen (I. G. Gazaryan, unpublished data) as electron acceptors in the NADH dehydrogenase reaction. All of these substrates have different protonation profiles, which eliminates substrate protonation as a significant contributor to the different pH activity curves observed for DCPIP and LA. Another possible explanation is that protonation of enzyme thiols favors formation of fully reduced FAD, which is known to be the catalyst of all the NADH dehydrogenase reactions, over the charge-transfer complex. However, within the pH range from 5.5 to 7.5 no changes in the contribution of the charge transfer form of LADH to the spectrum of two-electron reduced LADH have been detected (36, 37). Therefore we examined the possibility that pH was changing the protein structure.

Gel Filtration – Fine performance liquid chromatography gel filtration of purified commercial preparations at pH 7.5 of pig heart LADH consistently showed a catalytically active protein shoulder with an estimated M_p, molecular mass, of 200 kDa (Figure 2*A*). The high molecular weight material displayed specific activity equal to the main peak and SDS-PAGE indicated only the presence of LADH protein monomers. Re-injection of the tetramer peak resulted only in a dimer peak (not shown). The relative abundance of the high molecular weight form was dependent on the initial concentration of the protein, but never exceeded 5%. It is likely that this shoulder corresponds to the

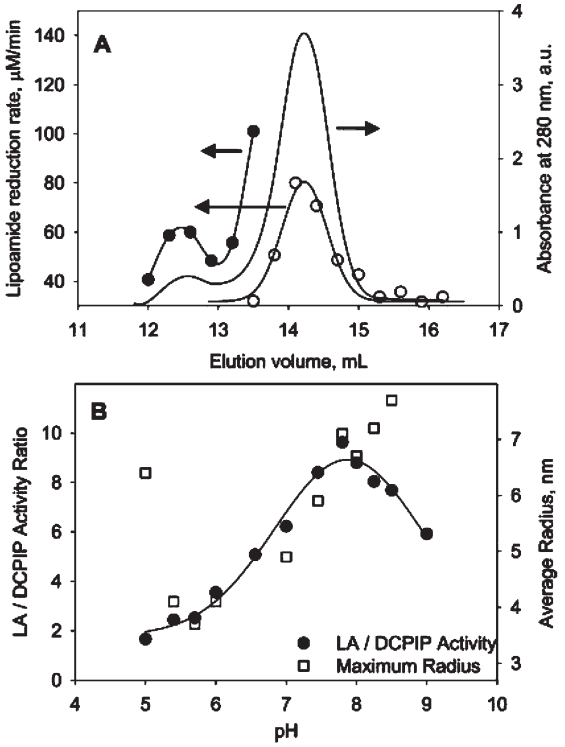

Figure 2. Characterization of LADH subunit association. ***A***, fast protein liquid chromatography of porcine heart LADH on a Superdex 200 column equilibrated with 0.2 M Tris-HCl buffer, pH 7.5. Absorbance profile is shown with a *solid line*. The activity in enzyme fractions was measured in the reaction of lipoamide reduction by NADH initiated by the addition of a LADH aliquot providing either 300-(•) or 1000-fold (○) dilution of the collected enzyme in the assay mixture (experimental conditions under "Materials and Methods"). ***B***, determination of hydrodynamic ratio of LADH by dynamic light scattering. *Open squares* (□) indicate the value of R_h determined at different pH values for 8 μM LADH solution. Buffer conditions are as described in the legend to Figure 1. *Closed circles* (•) are the ratio of LA specific activity divided by DCPIP specific activity at each pH. The *line* is inserted as a guide to the activity ratio dependence.

tetrameric form of LADH because of the M_p value and the presence of lipoamide dehydrogenase activity.

Dynamic Light Scattering – Quasielastic or DLS monitors time-dependent fluctuations in the intensity of light scattered by macromolecular solutions. Intensity fluctuations are because of local changes in the concentration of macromolecules responsible for scattering light. Analysis of these fluctuations in the time domain (autocorrelation function) provides a method for the determination of the diffusion rates of macromolecules. The latter can be converted into a hydrodynamic radius, R_h, assuming spherically shaped macromolecules and accounting for the solvent viscosity and temperature (38). The hydrodynamic radius of proteins has consistently been observed to be larger than the protein radius derived from crystal structures. This discrepancy has been attributed to many factors including "bound" water (hydration shells), frictional coupling to solvent, and deviation from spherical shape (39). DLS has been used successfully to detect changes in subunit association and aggregation in many systems.

DLS was employed to assess possible changes of subunit association with varying pH. The autocorrelation function was analyzed to yield the distribution of hydrodynamic radii at each pH value. The average (most probable) hydrodynamic radius reaches a minimum of 3.7 nm at pH 5.7 and increases monotonically to 7.8 nm at pH 8.5 (Figure 2*B*). Below pH 5.4 a time-dependent increase in the hydrodynamic radius was observed, consistent with aggregation. It has been noted that pig heart LADH is

unstable below pH 5.5 (37). For the purpose of comparison, data from Figure 1 were re-plotted as the ratio of LA and DCPIP activities (Figure 2*B*, *closed circles*). The shift toward greater subunit association over the pH interval from 5.7 to 8.0 is accompanied by increasing preference for LA over DCPIP activity. Above pH 8, the preference for the LA reaction begins to decline, whereas the hydrodynamic radius continues to increase. Thus, the pH changes in the reaction specificity of pig heart LADH correlate with the changes in the oligomeric state.

Reverse Micelles – The gel filtration and DLS data presented above suggest the existence of multiple oligomeric states of LADH. The pH behavior in enzyme and hydrodynamic studies suggests that enzyme activity may vary in correlation with association state. To examine this possibility in greater detail, structure-reactivity studies were initiated using the well established system of reverse micelles as a media for enzymatic reactions (40–46). Reverse micelles are self-forming and thermodynamically stable aggregates in which micelle size can be varied over a wide range by changing the surfactant hydration degree (w_o), *i.e.* the molar ratio water/surfactant in the system. Entrapping enzymes in nanocontainers composed of surfactant or lipid molecules in organic solvents gives an advantage in elucidation of structure-function relationships for supramolecular complexes (42–46). Enzymes display peaks in catalytic activity when the inner volume of the micelle closely matches the volume of the entrapped protein (42–46).

The diaphorase activity of LADH was used to detect oligomeric forms in reverse micelles because all enzyme forms, including monomer, retain this activity. In contrast, it was reported that LADH monomer does not display lipoamide dehydrogenase activity in aqueous solution (47, 48). DCPIP was chosen as a substrate because it is readily soluble in both aqueous and micellar (organic) media.

The catalytic activity of enzymes entrapped in reverse micelles display a bell-shaped dependence on the micelle size (see Refs. 41, 46, and 49, and references therein). Maximum activity is observed at the hydration degree, w_o, where the size of a micelle is equal to that of the entrapped protein. It is thought that the close contact between surfactant shell and enzyme helps maintain the latter in the catalytically active conformation. In the case of oligomeric enzymes, the dependence of kinetic parameters on w_o shows peaks corresponding to each oligomeric form of an enzyme (49, 51–54).

A plot of the dependence of LADH catalytic activity on w_o at pH 7.5 shows a clearly evident peak at a hydration degree (w_o) of 19–20 and a less pronounced peak at a higher value of w_o for diaphorase activity (Figure 3, *curve 1*). Lipoamide dehydrogenase activity was observed as two peaks at w_o of 20 and 36–40 for Figure 3, *curve 2*. These profiles suggest trapping of two oligomeric forms of active LADH that display different ratios of lipoamide dehydrogenase and diaphorase activities. Because optimum enzyme activity is observed when the diameter of micelle inner cavity matches the protein diameter, $r_m = r_p$, the w_o values for the peaks can be used to calculate the molecular mass (Da) of "compact" spherical proteins according to the simple equation,

$$MP = (4\pi \rho_p N_A)/3 \times r_p^3 = (r_p/0.7)^3 \quad (3)$$

where r_p is the protein radius in Å, N_A is Avogadro's number, and ρ_p is protein density equal to 1.2 g/cm^3 for many proteins. Conversely, theoretical values of the optimal w_o for spherical proteins can be calculated by combining Equations 1 and 3 as follows (50).

$$w_0 = 0.47\,(M_p\,(\mathrm{Da}))^{1/3} - 2.67 \quad (4)$$

The molecular mass of LADH estimated from w_o = 19–20 (Figure 3) and Equation 3 is 100–114 kDa, which corresponds to the dimeric form of LADH. Higher molecular mass aggregates are suggested from the second broad peak for DCPIP activity at hydration degrees w_o = 30–40.

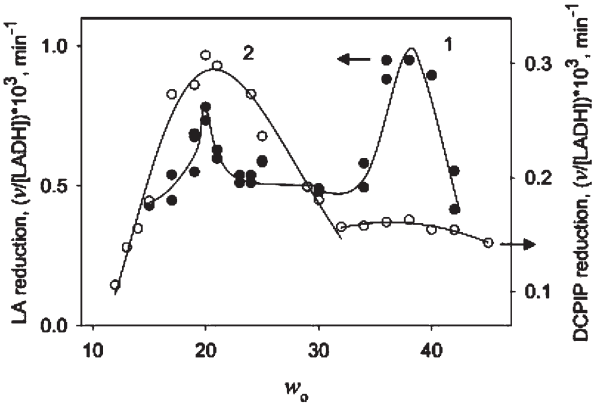

Figure 3. Dependence of the reaction rate (expressed as v/[LADH]) for DCPIP (*line 1* and *hollow circles*) and lipoamide (*line 2* and *solid circles*) reduction by NADH catalyzed by LADH in 50 mM Tris-HCl buffer, pH 7.5, in reverse micelles formed by 0.1 M AOT in octane on surfactant hydration degree, w_o (pH 7.5). Final concentrations of enzyme and substrates were 41 nM LADH, 0.1 mM NADH, and 2 mM LA for the lipoamide dehydrogenase reaction; and 300 nM LADH, 0.225 mM NADH, and 0.138 mM DCPIP for the diaphorase reaction. The rate of DCPIP reduction was recorded at 568 nm and the rate of NADH oxidation at 340 nm, both at 25 °C.

Kinetic Analysis – Both kinetic parameters (V_m and K_m) contribute to the overall LADH activity in the micellar system and in some cases the measured rate profile can be smoothed by their superposition. To avoid this difficulty the w_o dependence profile was determined for each individual parameter.

To justify determination of V_m and K_m, it was first necessary to establish that the micellar LADH system obeys Michaelis-Menten kinetics. Figure 4*A* illustrates that the reaction rate is proportional to the enzyme concentration used. Lineweaver-Burk plots of the diaphorase reaction for NADH (Figure 4*B*) and DCPIP (Figure 4*C*), at w_o equal 20 and 36, clearly demonstrate Michaelis-Menten kinetics. Figure 4*B* indicates that the kinetic parameters for NADH are almost independent of the hydration degree, which is in contrast to DCPIP (Figure 4*C*). These results together with similar data for the LA reaction (Figure 4, *D*–*F*) justify calculation of V_m and K_m parameters for all three substrates.

DCPIP concentration was varied in the presence of saturating NADH, which allowed the dependence of kinetic parameters on the hydration degree (w_o) to be calculated from plots similar to Figure 4*C*. Figure 5 illustrates that both V_m and K_m reach sharp maxima at w_o = 19 and 38 for both DCIP and LADH activities. The first optimum, as calculated above, corresponds to the molecular mass of dimeric LADH entrapped in micelles (~100 kDa). The second maximum at w_o = 38 corresponds to a hypothetical molecular mass ~634 kDa, assuming that the entrapped protein is spherical in shape (see Equations 1 and 3). This estimate corresponds to the maximum protein mass that can be accommodated within micelles of this hydration degree. However, if the protein shape is non-spherical (*e.g.* ellipsoid), the inner cavity of spherical micelle will only accommodate a protein with lower mass (50). As demonstrated below by sedimentation analysis, the actual mass of entrapped protein at w_o = 38 is ~200 ± 10 kDa, corresponding to LADH tetramer.

Close contact (leading to the increased rigidity of an enzyme molecule) with the surfactant shell helps maintain the enzyme in the catalytically active conformation, causing V_m to increase (higher catalytic activity). In addition, the increased rigidity of an entrapped enzyme often causes the K_m to increase (*i.e.* weaker substrate binding) (49, 50). The ratio of catalytic parameters, V_m/

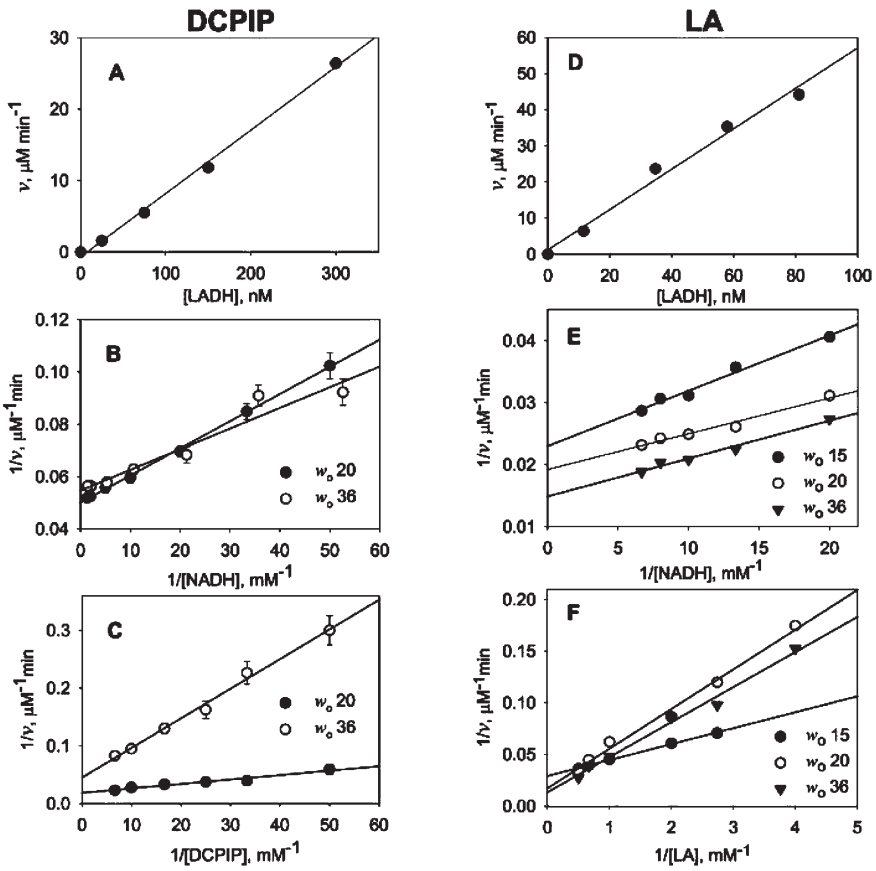

Figure 4. Michaelis-Menten kinetics of DCPIP reduction by NADH catalyzed by LADH in reverse micelles at different fixed hydration degrees, w_o. Reaction rate was recorded at 568 nm, 25 °C, in 0.1 M AOT-octane, 50 mM Tris-HCl buffer, pH 7.5 system. ***A***, dependence of the reaction rate on the concentration of LADH at fixed DCPIP (0.05 mM) and saturating NADH (0.2 mM) concentrations, w_o = 20. ***B***, Lineweaver-Burk plot of the diaphorase reaction rates at fixed concentrations of DCPIP (0.05 mM) and varied concentrations of NADH (0.02–0.75 mM), 300 nM LADH, w_o = 20, 36. ***C***, Lineweaver-Burk plot of the diaphorase reaction at a saturating concentration of NADH (0.2 mM) and varied concentrations of DCPIP (0.02–0.15 mM), and w_o = 20 and 36. LADH concentration for *B* and *C* was 300 nM.

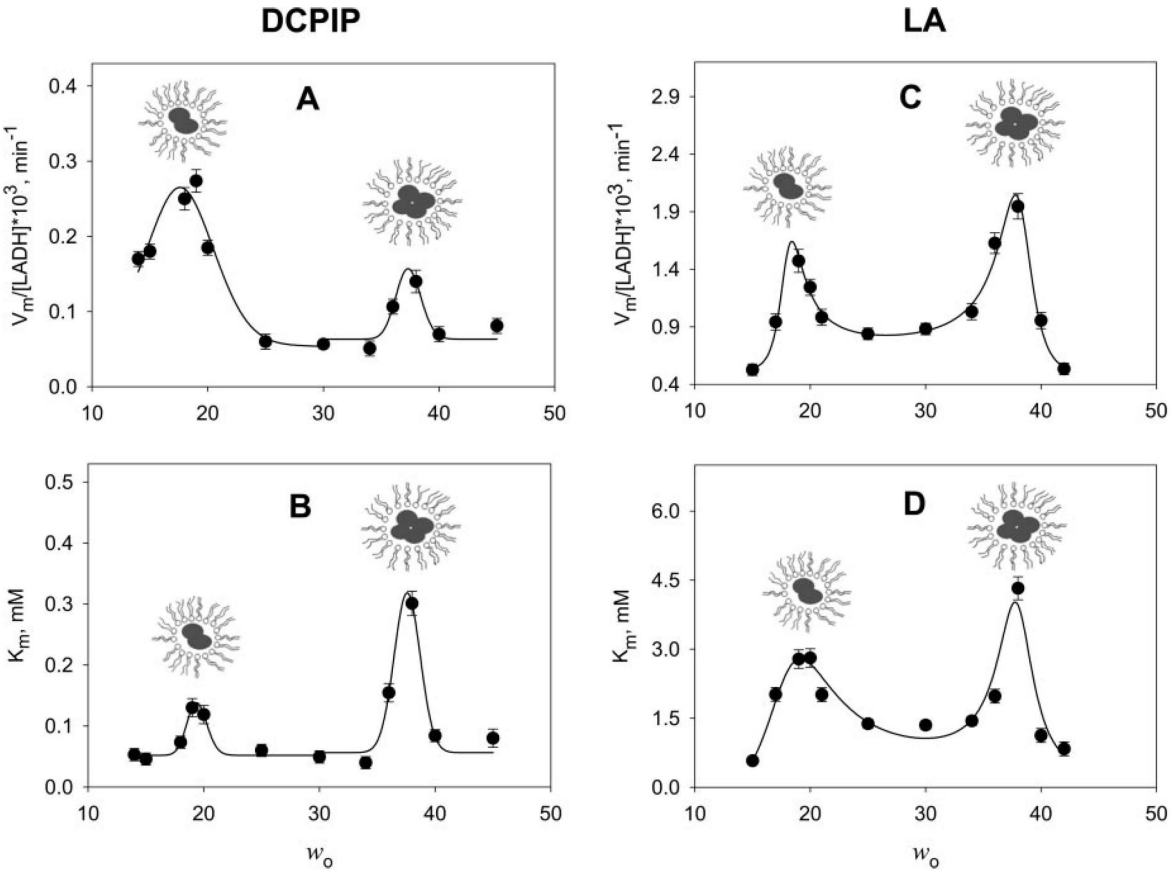

Figure 5. (below) Dependence of kinetic parameters (V_{max}/[LADH]; K_m) on surfactant hydration degree, w_o, for DCPIP or lipoamide reduction by NADH catalyzed by LADH in reverse micelles of AOT in octane at pH 7.5. ***A*** and ***B***, 300 nM LADH, 0.225 mM NADH, 0.02–0.15 mM DCPIP. ***C*** and ***D***, 41 nM LADH, 0.1 mM NADH, 0.25–2 mM LA (see Figure 3 for other experimental conditions).

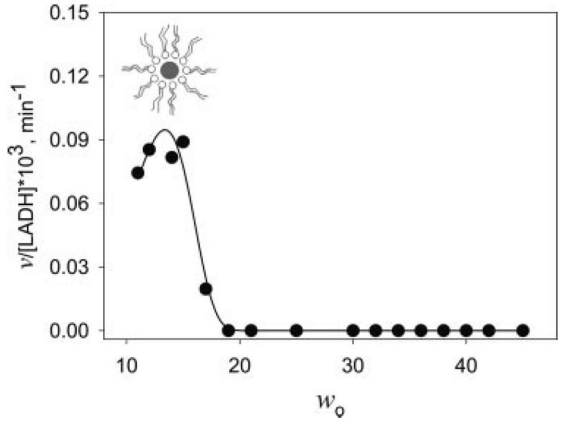

Figure 6. Dependence of the reaction rate (expressed as v/[LADH]) of DCPIP reduction by NADH catalyzed by 300 nM LADH in 25 mM citrate buffer, pH 5.8, in reverse micelles formed by 0.1 M AOT-octane on surfactant hydration degree, w_o. The rate of DCPIP reduction was recorded at 535 nm, 25 °C. Substrate concentrations were 0.225 mM NADH and 0.15 mM DCPIP.

K_m, governs the enzyme activity at each w_o value. This ratio remains unchanged for dimer and tetramer peaks of lipoamide dehydrogenase activity (Figure 5, *C* and *D*). In contrast, for the diaphorase reaction the tetrameric form is ~5 times less active than the dimeric one (Figure 5, *A* and *B*). This difference is consistent with the observed plateau for diaphorase activity at higher w_o corresponding to the tetrameric form (Figure 3).

DCPIP Activity at pH 5.8 – The dependence of LADH catalytic activity on w_o at pH 5.8 shows a single DCPIP activity optimum observed at a novel hydration degree, w_o = 15 (Figure 6). The estimated molecular mass of this entrapped LADH form is 54 kDa, which closely matches the known M_p of LADH monomer (52 kDa (47)).

Sedimentation Analysis – A direct method for the determination of the molecular mass of a protein entrapped in reverse micelles at a given w_o was developed in our laboratory (30, 31). The ultracentrifugation method, in which particles move under the centrifugal force and their concentration distribution over the length of a centrifuge tube is detected at varied times, is useful for the characterization of macromolecules. Using this method, it is possible to obtain information about the shape, molecular mass, and density of the macromolecules. In the case of empty AOT micelles a single, pronounced sedimentation boundary is observed, which indicates that the sedimenting micelles have uniform shape and molecular mass (30, 31). When protein-containing AOT micelles are introduced a second, faster sedimenting boundary (protein-containing micelles) is observed, whereas the sedimentation behavior of the light fraction (empty micelles) remains unchanged (30, 31). Comparison of the sedimentation rate of empty and protein-containing micelles can be used to determine the molecular masses of the entrapped proteins (30, 31), which avoids the necessity of applying the Svedberg equation to determine diffusion coefficients.

To illustrate this approach, sedimentation traces for LADH-containing micelles at w_o = 34, pH 7.5, are shown in Figure 7*A*. Two clear boundaries are observed. The lower boundary (slow sedimenting particles) corresponds to empty micelles. The sedimentation coefficients of empty micelles, plotted on the s_o line in *panels B* and *C*, are in agreement with those previously observed (30, 31).

The upper boundary (fast sedimenting particles) represents protein-containing micelles. *Panels B* and *C* (Figure 7) present the sedimentation coefficients of the fast sedimenting particles as a function of w_o at pH 7.5 and 5.8, respectively. Application of Equation 2 to the sedimentation data in Figure 7, *B* and *C*, allows estimation of M_p, the molecular mass of the protein incorporated into reverse micelles (Figure 7, *D* and *E*, respectively). The resulting M_p values for LADH-containing micelles at pH 7.5 are 100 ± 10 and 200 ± 10 kDa, at low and high hydration degrees, respectively, which closely matches the theoretical molecular mass of LADH dimer and tetramer. Figure 7*E* indicates the existence of a monomeric form of LADH at pH 5.8, at low values of w_o, in addition to dimer and tetramer at higher hydration degrees.

The sedimentation data presented in Figure 7, *panels C* and *E*, are consistent with the existence of LADH dimers and tetramers entrapped in reverse micelles at pH 5.8, despite the absence of detectable diaphorase activity corresponding to these species in Figure 6. It is important to note that DLS and sedimentation experiments were performed with the native, oxidized form of LADH (*i.e.* without substrate), whereas diaphorase activity measurements were done under reducing conditions, which is known to stimulate enzyme dissociation (22). The results of sedimentation analysis suggest that the equilibrium between LADH oligomeric forms is pH-sensitive, *i.e.* lowering the pH shifts the equilibrium toward the monomeric form (compare Figure 7, *D* and *E*).

Comparison with Structural Model – The availability of the pig heart LADH sequence (55) and the crystal structure coordinates for the tetrameric pea enzyme (56) made it possible to create models for the structures of monomeric, dimeric, and tetrameric pig heart LADH by means of homology modeling. As shown in Figure 8, the calculated tetramer model is asymmetric. The combining site for E3-binding protein (57) for one of the dimers (indicated by *arrows*) faces outward. In contrast, the corresponding face in the other dimer faces the dimer-dimer interface and is probably involved in stabilizing the interaction between dimers. It should be noted that the overall orientation of subunits is derived from the crystal structure and is unlikely to be greatly altered by homology modeling.

Table I summarizes the estimates of molecular radii derived from independent reversed micelle experiments and compares them with protein dimensions extracted from the model structures. The first group (*active*) of values are determined from kinetic experiments; the hydration degree (w_o) that resulted in optimal activity was converted into the enzyme radius (r_m). Second, the protein molecular mass (M_p) was determined from sedimentation velocity experiments. This mass was used to calculate a spherical radius (r_p) that represents the most *compact* protein conformation. Third, the range of w_o values in sedimentation experiments that was observed to contain each mass was interpreted as the actual *physical range* of radii assumed by each oligomeric form. Finally, molecular dimensions were computed from a structural *model* developed from reference crystal structures by the homology modeling method.

Examination of the tabulated results reveals several patterns. 1) The dimensions derived from the model for each oligomeric form always fall within the observed range of physical sizes, which provides partial validation of the model structure. 2) The *active* and *compact* structures have similar radii in the monomer (25–27 Å) and dimer (32–33 Å). 3) The *compact*, *active*, and *model* monomer structures all fall within the actual *physical range* at pH 5.8. In contrast, there is no physical evidence from sedimentation experiments of monomer formation at pH 7.5. Thus, no monomer activity is observed at pH 7.5 because none is formed. 4) The *compact* and *active* dimer structures (32–33 Å) fall within the actual *physical range* at pH 7.5 (26–48 Å), but not pH 5.8 (42–64 Å). This suggests that the *active* dimer shape is close to spherical in reverse micelles and that the elongated conformation of

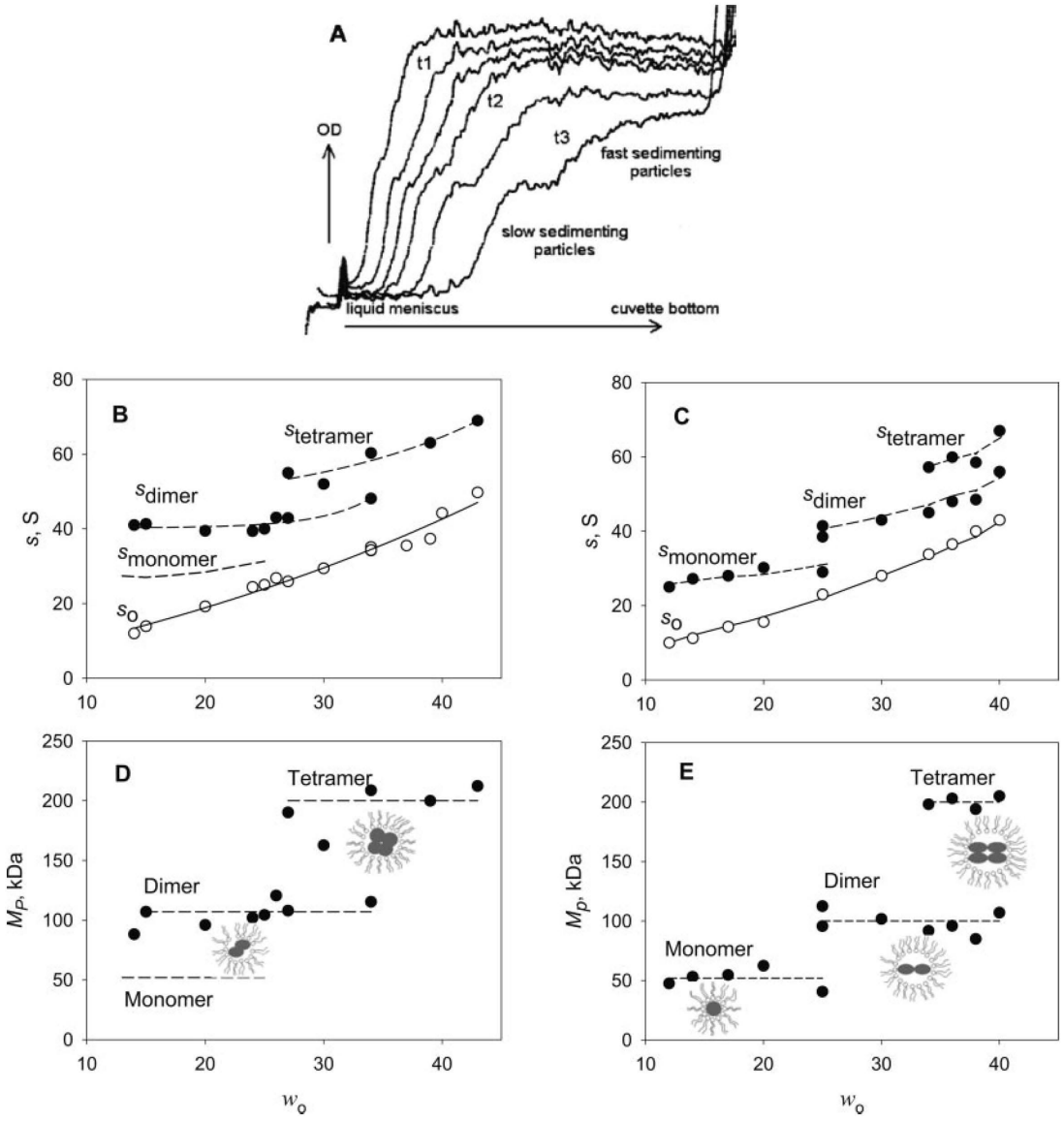

Figure 7. Sedimentation analysis of 5-10 μM LADH in 0.1 M AOT-octane reverse micelles (20 °C; 280 nm; 20,000 rpm). ***A***, typical sedimentation traces of LADH-containing 0.1 M AOT reverse micelles in octane at pH 7.5. The *uppermost* portion of the sedimenting boundaries correspond to the tetrameric form of LADH within reverse micelles at pH 7.5; w_o = 34. The *lowermost* portion of the boundaries correspond to the empty micelles. The *vertical arrow* indicates increasing LADH concentrations measured by absorbance at 280 nm (OD). The *horizontal axis* shows the distance between the liquid meniscus and the bottom of a cell. Each *curve* was recorded at a defined time ($t > t > t$). Total time course is 62 min. ***B*** and ***C***, dependence of sedimentation coefficients (*s*, S) of LADH-containing and empty reverse micelles on different hydration degrees at pH 7.5 (***B***) and 5.8 (***C***). *Solid lines* show the approximation of experimental sedimentation coefficients of empty micelles described by us (31). The *dashed lines* are computer simulations of predicted sedimentation coefficients using Equation 2 for protein containing micelles of hypothetic M_p 50, 100, and 200 kDa. The *symbols* correspond to observed sedimentation coefficients for LADH-containing (*closed circles* – •) and empty (*open circles* – ○) micelles. ***D*** and ***E***, molecular mass of LADH (kDa) within micelles calculated from experimental sedimentation coefficients of protein-containing micelles using Equation 2 at different hydration degrees, w_o. ***D***, pH 7.5. ***E***, pH 5.8. The *dashed lines* correspond to molecular masses of hypothetic proteins (M_p 50, 100, and 200 kDa).

that dimer at pH 5.8 is either catalytically incompetent or unstable upon reducing conditions used in the diaphorase reaction. Our observation of two different dimer conformations, *i.e.* compact and elongated, may correspond to the "non-dissociable" and "dissociable" LADH forms, respectively, observed more than 30 years ago (58) that were reported to be "structurally indistinguishable" (59). 5) In the case of tetramer, the *active* radius (61 Å) falls within the *physical range* determined from sedimentation experiments at pH 5.8 (55–64 Å) and pH 7.5 (42–70 Å). However, the *active* radius far exceeds the calculated radius (41 ± 1 Å) of a *compact* conformation. This indicates that the active tetramer is elongated, consistent with the *model* radius (60 Å). However, it is unclear why no diaphorase activity is observed for tetramer at pH 5.8.

Discussion

This study demonstrates that alterations in subunit association and protein conformation are correlated with changes in enzyme activity and reaction specificity. The novelty of the results presented lies is in the discovery of pH-driven equilibria between four LADH forms: tetramer, compact dimer, elongated dimer, and monomer. In addition, the results indicate that LADH dimer has an increased tendency to form protein-protein contacts at pH values found in the mitochondrial matrix under physiological conditions.

Below pH 6 the predominant *catalytically active* form of LADH is a monomer. It has been established that amino acid residues from both dimer subunits participate in formation of the

lipoamide active site (60). Therefore, monomer is not expected to be active in LA reduction. In contrast, NADH and DCPIP interact exclusively with the FAD catalytic site, which does not require participation of both subunits. Thus, conditions that favor dimer formation will favor the LA reaction, because catalysis requires dimeric enzyme. In addition, dimer formation directly disfavors DCPIP activity because LADH dimer is capable of forming a "charge transfer complex" (61), which has lower activity for DCPIP reduction than enzyme containing fully reduced FAD (I. G. Gazaryan *et al.*, manuscript in preparation).

The pH-sensitive equilibrium observed between LADH oligomeric forms suggests that lowered pH may facilitate rearrangement of LADH association among complexes within the mitochondrial matrix by relaxing the avidity of protein-protein interactions. A recent study estimates the matrix pH of polarized mitochondria in cells to be ~8 (2), which would favor dimer and tetramer forms of LADH. Loss of mitochondrial membrane potential would result in the lowering of matrix pH (cytosolic pH is ~6.8 (62)), shifting the equilibrium toward the monomeric enzyme form. Cytosolic acidification, which is associated with I/R, would contribute to further lowering of matrix pH. The consequence of this pH-induced shift in equilibrium would be to alter the ratio between diaphorase and lipoamide dehydrogenase activities. Figs. 3 and 5 demonstrate that compared with the dimer, dehydrogenase activity is increased and diaphorase activity decreased in the tetrameric form of LADH. Consistent with this trend, titration experiments indicate that diaphorase activity is most favored at about pH 5.8, whereas dehydrogenase activity is most favored at pH 7.5 (Figure 1).

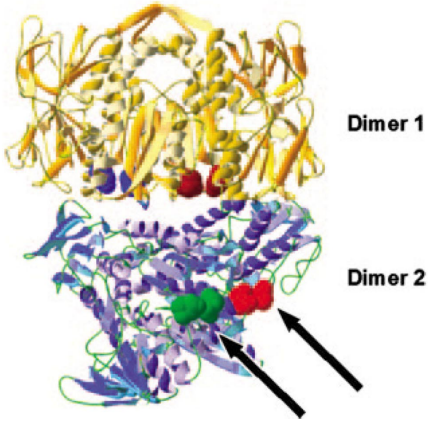

Figure 8. Tetrameric model for pig heart LADH obtained by homology modeling using garden pea LADH (Protein Data Bank code 1DXL [PDB]) as a template. Dimer 1 is in *yellow* and Dimer 2 is in *blue*, FAD not shown. *Arrows* mark the available contact site for E3-binding protein (residues Asp-350 and Glu-437 of each monomer) assigned by analogy with the structure of the PDH complex of *Bacillus stearother-mophilus* (57). These residues are shown in different colors for each subunit.

The observation of a stable LADH monomer that preserves its diaphorase activity in reverse micelles is novel. Previously, chemical cross-linking was the only procedure that allowed trapping the catalytically active LADH monomer (21). The fact that reverse micelles (or lipidic particles, in membrane terminology) can stabilize the monomeric enzyme form and make it catalytically competent for diaphorase activity should be considered when discussing the fate of mitochondria undergoing crystae remodeling, fission, and/or apoptosis under the conditions of oxidative stress.

Catalytically active monomer, dimer, and a novel tetramer forms of LADH were observed. All FAD-dependent thiol-disulfide oxidoreductases are thought to function as homodimers in solution. Tetrameric forms of *Spirulina maxima* and human glutathione reductases have been demonstrated in solution (63) and more recently a tetrameric form of garden pea LADH was observed in the crystallographic unit cell (56). Therefore, the tendency to form tetrameric structures may be considered as an inherent property of this family of flavin thiol-disulfide oxidoreductases.

Although the present study does not provide direct evidence about the structure of mitochondrial multienzyme complexes, it suggests that the reduced pH encountered during ischemia will destabilize LADH subunit self-association and LADH dimer interactions with other proteins. It is generally assumed that the complexes contain dimeric LADH; consideration of volume constraints in computer modeling suggests that the multienzyme structure could accommodate tetramer or dimer (64).

The ratio of the LADH to other components of the mitochondrial multienzyme complexes has not been settled experimentally (23, 65, 66). The likely reason for this uncertainty is that the ratio is not constant and varies in response to metabolic demands. An abundant pool of LADH, the terminal enzyme present in all of these complexes, is not bound into any multienzyme complexes (67). This suggests that alterations in the organization between LADH and other enzymatic partners may serve other purposes in addition to the regulation of energy metabolism. A recent report characterizes the involvement of E2 and E3 subunits linked to peroxiredoxin alkyl hydroperoxide reductase via a thioredoxin-like adaptor protein in *Mycobacterium tuberculosis* antioxidant defense (68). Similarly, recently discovered NO reduction by pig heart LADH yielding nitrate with the micromolar values of Michaelis-Menten constants suggests the possible involvement of LADH in antioxidant defense. The pH optimum of this reaction is near 6 (69), the same value that favors LADH diaphorase activity and dissociation from the multienzyme complexes.

Cytoplasmic acidification is a well known result of ischemia. Mitochondrial membrane potential can be maintained temporarily by consuming ATP generated from glycolysis. However, the

Table I. The comparison of molecular dimensions of LADH oligomeric forms obtained from direct experimental methods and computer modeling

LADH oligomeric forms	Kinetic experiments		Sedimentation experiments				Computer modeling	
	r_m from w_0 at V_m, K_m peaks (DCPIP)[a]	r_m from w_0 at V_m, K_m peaks (LA)[a]	*MP* calculated from S_p[b]	r_p calculated from M_p[c,d]	r_m range from w_0 (pH 5.8)[a]	r_m range from w_0 (pH 7.5)[a]	Model dimensions	Model radius (longest axis)
Monomer	27 Å[e]		50 ± 4 kDa[e]	25 ± 1 Å[e]	22–42 Å		60 × 60 × 60 Å	30 Å
Dimer	33	33	100 ± 10	32 ± 1	42–64	26–48 Å	95 × 65 × 60	48
Tetramer	61.0	61.0	200 ± 10	41 ± 1 (64 ± 1)[d]	55–64	42–70	120 × 100 × 80	60
Conformation	"Active"		"Compact"		"Physical range"		"Model"	

[a] The inner micellar cavity radius was calculated using Equation 1.
[b] The radius of the protein (r_p) was calculated from modified Equation 3.
[c] M_p was calculated by using Equation 2.
[d] The r_p was calculated as a radius of longest semiaxis of ellipsoid with relation between semiaxises: r : r : 2r.
[e] Monomer was observed at pH 5.8, no monomer was found at pH 7.5.

eventual loss of mitochondrial membrane potential upon ATP depletion will inevitably result in matrix acidification. The extent of matrix acidification will be further compounded because the matrix pH will equilibrate with the acidified cytoplasm. Our results suggest that the loss of mitochondrial membrane potential and lactic acidosis will have a dramatic effect on the structure and catalytic properties of energy-producing mitochondrial complexes that contain LADH. However, no studies have been performed yet to directly analyze the effect of pH on the structural organization of these complexes within mitochondria.

One possible consequence of pH-induced dissociation of LADH is the inactivation of pyruvate dehydrogenase, which is observed following I/R. LADH is attached to the complexes through the E3-binding domain of the E2 component (or an individual binding protein in the pyruvate dehydrogenase complex), which binds LADH dimer at the interface formed by both monomeric subunits. Lowering the matrix pH would be less favorable to higher-order association and will eventually destabilize the LADH dimer. Patel and Korotchkina (70) demonstrated that the activities of some PDHC kinases are stimulated by reduction of the lipoyl groups attached to the E2 subunit. Reduced pH may stimulate dissociation of LADH from PDHC, resulting in reduced lipoyl groups that are unable to cycle back to their oxidized form. Chronically reduced E2 will stimulate phosphorylation of E1α, resulting in reduced PDHC activity after ischemia, which can be reversed by treatment with dichloroacetate. Alternately, PDHC will be inactivated because of the loss of the E3 subunit. This second form of inactive PDHC will be more resistant to reactivation if subunit dissociation is followed by release of the FAD group or protein unfolding.

Acknowledgments

We thank Dr. Igor Ouporov for assistance with computer modeling. N. L. K. and V. A. S. thank Prof. Andrey V. Levashov for helpful critical comments.

References

1. Ghafourifar, P., and Richter, C. (1999) *Biol. Chem.* **380,** 1025–1028
2. Abad, M. F., Di Benedetto, G., Magalhaes, P. J., Filippin, L., and Pozzan, T. (2004) *J. Biol. Chem.* **279,** 11521–11529
3. Petronilli, V., Cola, C., and Bernardi, P. (1993) *J. Biol. Chem.* **268,** 1011–1016
4. Matsuyama, S., Llopis, J., Deveraux, Q. L., Tsien, R. Y., and Reed, J. C. (2000) *Nat. Cell Biol.* **2,** 318–325
5. Das, D. K., and Maulik, N. (1996) *Exs* **76,** 155–173
6. Kobayashi, K., and Neely, J. R. (1983) *J. Mol. Cell. Cardiol.* **15,** 359–367
7. Zaidan, E., and Sims, N. R. (1993) *J. Cereb. Blood Flow Metab.* **13,** 98–104
8. Cardell, M., Koide, T., and Wieloch, T. (1989) *J. Cereb. Blood Flow Metab.* **9,** 350–357
9. Bogaert, Y. E., Sheu, K. F., Hof, P. R., Brown, A. M., Blass, J. P., Rosenthal, R. E., and Fiskum, G. (2000) *Exp. Neurol.* **161,** 115–126
10. Bogaert, Y. E., Rosenthal, R. E., and Fiskum, G. (1994) *Free Radic. Biol. Med.* **16,** 811–820
11. Lemasters, J. J., Nieminen, A. L., Qian, T., Trost, L. C., Elmore, S. P., Nishimura, Y., Crowe, R. A., Cascio, W. E., Bradham, C. A., Brenner, D. A., and Herman, B. (1998) *Biochim. Biophys. Acta* **1366,** 177–196
12. Racey-Burns, L. A., Burns, A. H., Summer, W. R., and Shepherd, R. E. (1989) *Life Sci.* **44,** 2015–2023
13. Assaf, H. M., Ricci, A. J., Whittingham, T. S., LaManna, J. C., Ratcheson, R. A., and Lust, W. D. (1990) *Metab. Brain Dis.* **5,** 143–154
14. Patel, M. S., and Roche, T. E. (1990) *FASEB J.* **4,** 3224–3233
15. Arscott, L. D., Gromer, S., Schirmer, R. H., Becker, K., and Williams, C. H., Jr. (1997) *Proc. Natl. Acad. Sci. U. S. A.* **94,** 3621–3626
16. Thorpe, C., and Williams, C. H., Jr. (1976) *J. Biol. Chem.* **251,** 3553–3557
17. Gazaryan, I. G., Krasnikov, B. F., Ashby, G. A., Thorneley, R. N., Kristal, B. S., and Brown, A. M. (2002) *J. Biol. Chem.* **277,** 10064–10072
18. Reed, J. K. (1973) *J. Biol. Chem.* **248,** 4834–4839
19. Leichus, B. N., and Blanchard, J. S. (1992) *Biochemistry* **31,** 3065–3072
20. Nakamura, M., and Yamazaki, I. (1972) *Biochim. Biophys. Acta* **267,** 249–257
21. Tsai, C. S., Templeton, D. M., and Wand, A. J. (1981) *Arch. Biochem. Biophys.* **206,** 77–86
22. van Berkel, W. J., Regelink, A. G., Beintema, J. J., and de Kok, A. (1991) *Eur. J. Biochem.* **202,** 1049–1055
23. Zhou, Z. H., McCarthy, D. B., O'Connor, C. M., Reed, L. J., and Stoops, J. K. (2001) *Proc. Natl. Acad. Sci. U. S. A.* **98,** 14802–14807
24. Popov, V. O., Gazarian, I. G., Egorov, A. M., and Berezin, I. V. (1985) *Biochim. Biophys. Acta* **827,** 466–471
25. Massey, V., Hofmann, T., and Palmer, G. (1962) *J. Biol. Chem.* **237,** 3820–3828
26. Ghisla, S., Massey, V., Lhoste, J. M., and Mayhew, S. G. (1974) *Biochemistry* **13,** 589–597
27. Eicke, H. F. (1980) *Top. Curr. Chem.* **87,** 85–145
28. Kotlarchyk, M., Huang, J. S., and Chen, S.-H. (1985) *J. Phys. Chem.* **89,** 4382–4386
29. Kohling, R., Woenckhaus, J., Klyachko, N. L., and Winter, R. (2002) *Langmuir* **18,** 8626–8632
30. Levashov, A. V., Khmelnitsky, Y. L., Klyachko, N. L., Chernyak, V., and Martinek, K. (1981) *Anal. Biochem.* **118,** 42–46
31. Levashov, A. V., Khmelnitsky, Y. L., Klyachko, N. L., Chernyak, V. Y., and Martinek, K. (1982) *J. Colloid Interface Sci.* **88,** 444–457
32. Altschul, S. F., Madden, T. L., Schaffer, A. A., Zhang, J., Zhang, Z., Miller, W., and Lipman, D. J. (1997) *Nucleic Acids Res.* **25,** 3389–3402
33. Thompson, J. D., Higgins, D. G., and Gibson, T. J. (1994) *Nucleic Acids Res.* **22,** 4673–4680
34. Guex, N., Diemand, A., and Peitsch, M. C. (1999) *Trends Biochem. Sci.* **24,** 364–367
35. Guex, N., and Peitsch, M. C. (1997) *Electrophoresis* **18,** 2714–2723
36. Matthews, R. G., and Williams, C. H., Jr. (1976) *J. Biol. Chem.* **251,** 3956–3964
37. Sahlman, L., and Williams, C. H., Jr. (1989) *J. Biol. Chem.* **264,** 8033–8038
38. Kazakov, S. V., Galaev, I. Y., and Mattiasson, B. (2002) *Int. J. Thermophys.* **23,** 161–173
39. Halle, B., and Davidovic, M. (2003) *Proc. Natl. Acad. Sci. U. S. A.* **100,** 12135–12140
40. Martinek, K., Levashov, A. V., Khmelnitsky, Y. L., Klyachko, N. L., and Berezin, I. V. (1982) *Science* **218,** 889–891
41. Martinek, K., Levashov, A. V., Klyachko, N., Khmelnitski, Y. L., and Berezin, I. V. (1986) *Eur. J. Biochem.* **155,** 453–468
42. Luisi, P. L., Giomini, M., Pileni, M. P., and Robinson, B. H. (1988) *Biochim. Biophys. Acta* **947,** 209–246
43. Oldfield, C. (1994) *Biotechnol. Genet. Eng. Rev.* **12,** 255–327
44. de Gomez-Puyou, T. M., and Gomez-Puyou, A. (1998) *Crit. Rev. Biochem. Mol. Biol.* **33,** 53–89
45. Orlich, B., and Schomacker, R. (2002) *Adv. Biochem. Eng. Biotechnol.* **75,** 185–208
46. Klyachko, N. L., and Levashov, A. V. (2003) *Curr. Opin. Colloid Interface Sci.* **8,** 179–186
47. Visser, J., and Veeger, C. (1968) *Biochim. Biophys. Acta* **159,** 265–275
48. van Berkel, W. J., Benen, J. A., and Snoek, M. C. (1991) *Eur. J. Biochem.* **197,** 769–779
49. Levashov, A. V., and Klyachko, N. L. (2001) *Russ. Chem. Bull.* **50,** 1718–1732
50. Klyachko, N. L., Pshezhetsky, A. V., Kabanov, A. V., Vakula, S. V., Martinek, K., and Levashov, A. V. (1990) *Biol. Membrany (Russ.)* **7,** 467–472
51. Kabanov, A. A., Nametkin, S. N., Klyachko, N. L., and Levashov, A. V. (1991) *FEBS Lett.* **278,** 143–146
52. Kabanov, A. V., Klyachko, N. L., Nametkin, S. N., Merker, S., Zaroza, A. V., Bunik, V. I., Ivanov, M. V., and Levashov, A. V. (1991) *Protein Eng.* **4,** 1009–1017
53. Martinek, K., Klyachko, N. L., Kabanov, A. V., Khmelnitsky Yu, L., and Levashov, A. V. (1989) *Biochim. Biophys. Acta* **981,** 161–172
54. Gazaryan, I. G., Klyachko, N. L., Dulkis, Y. K., Ouporov, I. V., and Levashov, A. V. (1997) *Biochem. J.* **328**, 643–647
55. Ross, J., Reid, G. A., and Dawes, I. W. (1988) *J. Gen. Microbiol.* **134**, 1131–1139
56. Faure, M., Bourguignon, J., Neuburger, M., MacHerel, D., Sieker, L., Ober, R., Kahn, R., Cohen-Addad, C., and Douce, R. (2000) *Eur. J. Biochem.* **267,** 2890–2898
57. Mande, S. S., Sarfaty, S., Allen, M. D., Perham, R. N., and Hol, W. G. (1996) *Structure* **4,** 277–286
58. v Muiswinkel-Voetberg, H., Visser, J., and Veeger, C. (1973) *Eur. J. Biochem.* **33,** 265–270
59. v Muiswinkel-Voetberg, H., and Veeger, C. (1973) *Eur. J. Biochem.* **33,** 271–278
60. Toyoda, T., Suzuki, K., Sekiguchi, T., Reed, L. J., and Takenaka, A. (1998) *J. Biochem. (Tokyo)* **123,** 668–674
61. Wilkinson, K. D., and Williams, C. H., Jr. (1979) *J. Biol. Chem.* **254,** 852–862
62. Awaji, T., Hirasawa, A., Shirakawa, H., Tsujimoto, G., and Miyazaki, S. (2001) *Biochem. Biophys. Res. Commun.* **289,** 457–462
63. Rendon, J. L., and Mendoza-Hernandez, G. (1989) *Arch. Biochem. Biophys.* **268,** 255–263
64. Raddatz, G., and Bisswanger, H. (1997) *J. Mol. Model* **3,** 423–433
65. de Kok, A., Hengeveld, A. F., Martin, A., and Westphal, A. H. (1998) *Biochim. Biophys. Acta* **1385,** 353–366
66. Aevarsson, A., Seger, K., Turley, S., Sokatch, J. R., and Hol, W. G. (1999) *Nat. Struct. Biol.* **6,** 785–792
67. Matuda, S., and Saheki, T. (1982) *J. Biochem. (Tokyo)* **91,** 553–561
68. Bryk, R., Lima, C. D., Erdjument-Bromage, H., Tempst, P., and Nathan, C. (2002) *Science* **295,** 1073–1077
69. Igamberdiev, A. U., Bykova, N. V., Ens, W., and Hill, R. D. (2004) *FEBS Lett.* **568,** 146–150
70. Korotchkina, L. G., and Patel, M. S. (2001) *J. Biol. Chem.* **276,** 37223–37229